Table 3 Logistic regression model for febrile neutropenia (N = 200)

Variable	Regression coefficient (SE)	p
Area under the plasma concentration versus time curve (AUC) (mg*h/L)	1.29 (0.174)	<0.001
Performance status* (PS*) (0 for PS 0/1 or 1 for PS 2/3)	1.41 (0.311)	<0.001
Intercept	−3.52 (0.434)	<0.001

AUC, area under the plasma concentration versus time curve

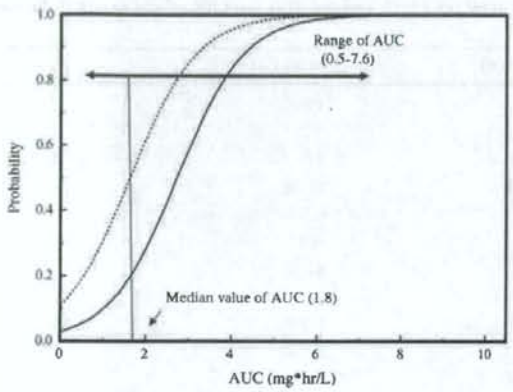

Fig. 1 A solid curve represents the probability of FN predicted from Eq. 2 at various AUC when performance status factor (PS*) was set at 0. A dotted curve represents the probability of FN predicted from Eq. 2 at various AUC when PS* was set at 1

all samples were converged normally, and AUC and PS* remained significant in the model for 195 samples. On the other hand, only AUC remained significant in the model for 5 samples. The area under an ROC curve of 200 samples (using bootstrapping) was calculated to be 0.85 as a mean value, with a CV (%) of 2.5. From these lines of evidence, this model was implied to have robustness and a good ability to discriminate between patients with and without fever.

Discussion

The population PK parameters and their interindividual variability of docetaxel in Japanese cancer patients have been reported [17]. In this study, the probability of FN occurrence was further investigated using the same patient population. Bruno et al. [14] reported that the AGP and CL of docetaxel are related with the risk of FN occurrence, using a logistic regression analysis for subjects in Europe and Western and USA. In this study, a stepwise logistic regression analysis was performed to evaluate the risk of FN occurrence using clinical data taken from Japanese

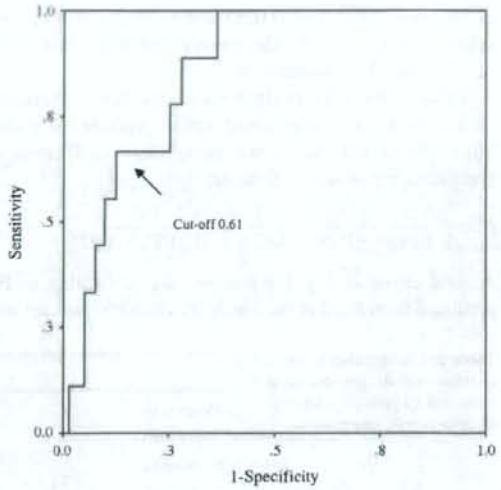

Fig. 2 Receiver-operating-characteristic (ROC) curve for the probability of febrile neutropenia predicted from this model in differentiating between those patients with and without febrile neutropenia

Table 4 Predictive performance of logistic regression model[a]

Group		Observed	
		Fever (+)	Fever (−)
Predicted	Fever (+)	6	25
	Fever (−)	3	166

[a] Cut-off value = 0.61

cancer patients treated with docetaxel, for the first time. Bruno et al [14], who studied the docetaxel-induced FN occurrence, reported the rate of FN as 4.7%, which is close to the result of our study. On the other hand, the rate of FN was reportedly higher (20–40%) in other cancer chemotherapy such as CHOP and ACVBP regimens for patients with non-Hodgkin's lymphoma [15, 16].

Figure 1 shows that when the patients with PS* classed at 1 received doses which provide the median value of AUC (1.8 mg*h/L) in this study, the probability of FN occurrence at PS* = 1 is expected to increase 2.5-fold as compared with that at PS* = 0.

From Table 4, the predictive value of fever (+), calculated as true positive/(true positive + false positive = 6/(6 + 25) = 0.19. This implies that the predict performance of the Eq. 2 is not high enough. In contrast, the predictive value of fever (−) was calculated as true negative/(true negative + false negative) = 166/(166 + 3) = 0.98. This implies that FN may not occur when the probability of FN occurrence calculated by Eq. 2 is less than 0.61. To

Table 5 Comparison the two groups where the dose ≤ cut-off dose and dose > cut-off dose[a]

Group	Dose ≤ cut-off dose[b]	Dose > cut-off dose[b]
Fever (−)	166	25
Fever (+)	3	6

[a] $p = 0.001$ (Fisher's exact test)

[b] Cut-off dose was a value which provided that the probability of febrile neutropenia was 0.61

support this hypothesis, Fisher's exact test for FN frequency was employed to compare the group administered with doses (normalized by body surface area (BSA)) more than the cut-off dose ($D_{\text{cut-off}}$, i.e. the dose which provides the FN probability of 0.61) with the group administered with doses less than $D_{\text{cut-off}}$. $D_{\text{cut-off}}$ was finally calculated as

$$D_{cut-off} = \frac{(3.02 - 1.09 \cdot \text{PS}^{*}) \cdot \text{CL}}{\text{BSA}} \quad (3)$$

where CL was given by a Bayesian post hoc analysis of the population PK model. As a result, the group administered with doses more than $D_{\text{cut-off}}$ showed a significantly higher frequency of FN ($p = 0.001$; Table 5). This indicates that patients administered with doses more than $D_{\text{cut-off}}$ tend to exhibit FN. In other words, the $D_{\text{cut-off}}$ calculated from Eq. 3 may be considered as a criterion when physicians do dose-adjustment to avoid FN occurrence. However, the condition used to decide dose of docetaxel using Eq. 3 is merely a reflection of toxicity associated with FN, but clinical efficacy (tumor regression) should also be taken into account in the clinical settings.

In the previous phase II study [14], the dose used was constant and was not changed, whereas in this study the dose was adjusted due to liver failure and/or prior chemotherapy because the patients have been treated under routine oncology practice. This conditional difference may be the reason why significant covariates were different between that trial and the present results of a logistic regression analysis for FN occurrence.

In conclusion, an equation was developed to predict the probability of FN occurrence in Japanese patients treated with docetaxel. This equation, which incorporates AUC and PS* as significant covariates, may therefore be useful for selecting the appropriate dose in order to avoid the occurrence of FN.

Acknowledgments This study was supported in part by Grants-in-Aid from the Ministry of Health and Welfare, Japan.

References

1. Bodey GP, Buckley M, Sathe YS, Freireich EJ (1966) Quantitative relationships between circulating leukocytes and infection in patients with acute leukemia. Ann Intern Med 64:328–339
2. Pizzo PA (1993) Management of fever in patients with cancer and treatment-induced neutropenia. N Engl J Med 328:1323–1332
3. Smith GM, Leyland MJ, Farrell ID, Geddes AM (1988) A clinical, microbiological and pharmacokinetic study of ciprofloxacin plus vancomycin as initial therapy of febrile episodes in neutropenic patients. J Antimicrob Chemother 21:647–655
4. Klastersky J (1993) Febrile neutropenia. Curr Opin Oncol 5:625–632
5. Rubenstein EB, Rolston KV (1995) Outpatient treatment of febrile neutropenic patients with cancer. Eur J Cancer 31A:2–4
6. Kojima A, Shinkai T, Soejima Y, Okamoto H, Eguchi K, Sasaki Y, Tamura T, Oshita F, Ohe Y, Saijo N (1994) A randomized prospective study of imipenem-cilastatin with or without amikacin as an empirical antibiotic treatment for febrile neutropenic patients. Am J Clin Oncol 17:400–404
7. Carlson JW, Fowler JM, Saltzman AK, Carter JR, Chen MD, Mitchell SK, Dunn D, Carson LF, Adcock LL, Twiggs LB (1994) Chemoprophylaxis with oral ciprofloxacin in ovarian cancer patients receiving taxol. Gynecol Oncol 55(Pt 1):415–420
8. Sjöström J, Blomqvist C, Mouridsen H, Pluzanska A, Ottosson-Lönn S, Bengtsson NO, Ostenstad B, Mjaaland I, Palm-Sjövall M, Wist E, Valvere V, Anderson H, Bergh J (1999) Docetaxel compared with sequential methotrexate and 5-fluorouracil in patients with advanced breast cancer after anthracycline failure: a randomised phase III study with crossover on progression by the Scandinavian Breast Group. Eur J Cancer 35(8):1194–1201
9. Fossella FV, DeVore R, Kerr RN, Crawford J, Natale RR, Dunphy F, Kalman L, Miller V, Lee JS, Moore M, Gandara D, Karp D, Vokes E, Kris M, Kim Y, Gamza F, Hammershaimb L (2000) Randomized phase III trial of docetaxel versus vinorelbine or ifosfamide in patients with advanced non-small-cell lung cancer previously treated with platinum-containing chemotherapy regimens. The TAX 320 Non-Small Cell Lung Cancer Study Group. J Clin Oncol 18(12):2354–2362. Erratum in: J Clin Oncol. 2004 Jan 1 22(1): 209
10. Vasey PA (2003) Role of docetaxel in the treatment of newly diagnosed advanced ovarian cancer. J Clin Oncol 21(10 Suppl):136s–144s
11. Dreyfuss AI, Clark JR, Norris CM, Rossi RM, Lucarini JW, Busse PM, Poulin MD, Thornhill L, Costello R, Posner MR (1996) Docetaxel: an active drug for squamous cell carcinoma of the head and neck. J Clin Oncol 14(5):1672–1678
12. Sulkes A, Smyth J, Sessa C, Dirix LY, Vermorken JB, Kaye S, Wanders J, Franklin H, LeBail N, Verweij J (1994) Docetaxel (Taxotere) in advanced gastric cancer: results of a phase II clinical trial. EORTC Early Clinical Trials Group. Br J Cancer 70(2):380–383
13. Tannock IF, de Wit R, Berry WR, Horti J, Pluzanska A, Chi KN, Oudard S, Theodore C, James ND, Turesson I, Rosenthal MA, Eisenberger MA; TAX 327 Investigators (2004) Docetaxel plus prednisone or mitoxantrone plus prednisone for advanced prostate cancer. N Engl J Med 351(15):1502–1512
14. Bruno R, Hille D, Riva A, Vivier N, ten Bokkel Huinnink WW, van Oosterom AT, Kaye SB, Verweij J, Fossella FV, Valero V, Rigas JR, Seidman AD, Chevallier B, Fumoleau P, Burris HA, Ravdin PM, Sheiner LB (1998) Population pharmacokinetics/pharmacodynamics of docetaxel in phase II studies in patients with cancer. J Clin Oncol 16:187–196
15. Blay JY, Chauvin F, Le Cesne A, Anglaret B, Bouhour D, Lasset C, Freyer G, Philip T, Biron P (1996) Early lymphopenia after cytotoxic chemotherapy as a risk factor for febrile neutropenia. J Clin Oncol 14(2):636–643
16. Intragumtornchai T, Sutheesophon J, Sutcharitchan P, Swasdikul D (2000) A predictive model for life-threatening neutropenia and febrile neutropenia after the first course of CHOP chemotherapy

in patients with aggressive non-Hodgkin's lymphoma. Leuk Lymphoma 37(3–4):351–360
17. Ozawa K, Minami H, Sato H (2007) Population pharmacokinetic-pharmacodynamic analysis for the time courses of docetaxel-induced neutropenia in Japanese cancer patients. Cancer Sci 98:1985–1992
18. Vergniol J, Bruno R, Montay G, Frydman A (1992) Determination of Taxotere in human plasma by a semi-automated high-performance liquid chromatographic method. J Chromatogr 582:273–278
19. Efron B, Tibshirani R (1986) Bootstrap methods for standard errors, confidence intervals, and other measures of statistical accuracy. Stat Sci 1:54–75
20. Harrell Jr FE, Lee KL, Mark DB (1996) Mulitvariable prognostic models: issues in developing models, evaluating assumptions and adequacy, and measuring and reducing errors. Stat Med 15:361–387

Lung Cancer (2008) 61, 195–201

available at www.sciencedirect.com

ScienceDirect

journal homepage: www.elsevier.com/locate/lungcan

Lung cancer screening—Comparison of computed tomography and X-ray

Ayako Fujikawa[a], Yuichi Takiguchi[a,*], Satoko Mizuno[a], Takahiro Uruma[a], Kiminori Suzuki[b], Keiichi Nagao[a], Mafumi Niijima[c], Hidenori Edo[c], Mitsunori Hino[d], Takayuki Kuriyama[a]

[a] *Department of Respirology, Graduate School of Medicine, Chiba University, 1-8-1, Inohana, Chuo-ku, Chiba 260-8670, Japan*
[b] *Chiba Foundation for Health Promotion & Disease Prevention, 32-14, Shin-Minato, Mihama-ku, Chiba 261-0002, Japan*
[c] *Department of Internal Medicine, Narita Red Cross Hospital, 90-1, Iida, Narita 286-8523, Japan*
[d] *Department of Internal Medicine, Nippon Medical School Chiba Hokusoh Hospital, 1715, Kamakari, Imba, Imba-gun 270-1694, Japan*

Received 21 October 2007; received in revised form 6 December 2007; accepted 11 December 2007

KEYWORDS
Lung cancer;
Computed tomography;
Mass screening;
Early detection;
Morbidity;
Mortality

Summary Recent studies on lung cancer screening with CT disclosed a discrepancy between its efficiency in detecting early lung cancer and a lack of proof for decreasing mortality from lung cancer. The present study, in a city in Japan where an X-ray screening program is provided, bi-annual CT screening was performed for X-ray screening negative subjects for 4 years. Ten patients with lung cancer were detected among 22,720 person-year subjects (0.044%) through the X-ray screening. Among the X-ray screening-negative subjects, 3305 subjects participated in a CT screening program resulting in the detection of 15 patients with lung cancer (0.454%). All 15 cases detected by CT screening and 5 of the 10 cases detected by X-ray screening were at stage IA. In respect of gender, histological type and CT findings, patients detected by CT screening had a better prognostic profile than those detected by X-ray screening. Survival was significantly better in the former than the latter, both in its entirety comparison and in a comparison limited to patients who underwent surgery. In conclusion, CT screening might have the potential to detect lung cancer with good prognostic factors not limited to early detection. Sufficiently long follow-up time, therefore, would be required to evaluate the efficacy for decreasing lung cancer mortality with CT screening.

* Corresponding author at: Department of Respirology (B2), Graduate School of Medicine, Chiba University, 1-8-1, Inohana, Chuo-ku, Chiba 260-8670, Japan. Tel.: +81 43 226 2577; fax: +81 43 226 2176.
E-mail addresses: wadabun@fa2.so-net.ne.jp (A. Fujikawa), takiguchi@faculty.chiba-u.jp (Y. Takiguchi), sato5kg@yahoo.co.jp (S. Mizuno), uruma-t@umin.ac.jp (T. Uruma), kimi.suzuki@nifty.com (K. Suzuki), nagaoke@faculty.chiba-u.jp (K. Nagao), mafumi@naritasekijyuji.jp (M. Niijima), mosquito650he@docomo.ne.jp (H. Edo), hino@nms.ac.jp (M. Hino), kuriyama@faculty.chiba-u.jp (T. Kuriyama).

0169-5002/$ – see front matter © 2007 Elsevier Ireland Ltd. All rights reserved.
doi:10.1016/j.lungcan.2007.12.010

1. Introduction

Lung cancer is the leading cause of cancer death in many countries worldwide. Hope of decreasing death from lung cancer by early detection has encouraged studies for lung cancer screening by chest X-ray [1–4], sputum cytology and low-dose spiral computed tomography (CT) [5–13].

Recently, a large scale study on lung cancer screening by CT (International Early Lung Cancer Action Program, or I-ELCAP) resulted in a diagnosis of lung cancer in 484 participants out of 31,567 asymptomatic persons at risk for lung cancer, a high ratio of clinical stage I of 85% in the diagnosed patients, and a high estimated 10-year survival rate of 88% in the subgroup with clinical stage I lung cancer, confirming the previous reports on CT screening [10]. On the other hand, another international study failed to show a decline in advanced lung cancer diagnoses and lung cancer deaths by CT screening when compared with estimated numbers by means of 2 prediction models, although it again disclosed significant efficacy in the early detection of lung cancer [14], revealing a discrepancy between the studies. Clarifying the characteristics of lung cancer detected by CT screening may help to explain this discrepancy. The present study, performed in a single region, compared the results of lung cancer screenings by low-dose CT with those by conventional chest X-ray in terms of efficacy and the characteristics of the detected lung cancers.

2. Materials and methods

2.1. Study region and subject recruitment

The study was conducted in an anonymous city located in a suburb in Chiba prefecture next to Tokyo, Japan. The municipal office has, for decades, provided its residents older than 40 years with an annual health-screening program including chest X-ray. All subjects participating in this program, on the day of the chest X-ray screening, were informed of the free-of-charge and research-based low-dose CT screening program to take place at a later date, together with its potential benefits and risks. Those who gave their written informed consent for the study became candidates for enrolling in the CT screening for lung cancer. Subjects who had abnormalities detected on the basis of the X-ray screening, and were judged to require further examinations, were excluded from enrollment in the CT screening program. New subjects were recruited every year for each screening. With encouragement, repeat of the screening at the next opportunity depended on the individual's will.

2.2. Lung cancer screening by chest X-ray and CT

For screening with X-ray, images in 10×10 cm miniature radiograms were obtained with mobile X-ray equipment (Model MXO-15B, Toshiba Medical Systems Co., Otawara, Japan) on X-ray film rolls (X-ray film HX, Konica Minolta Holdings, Inc., Tokyo, Japan) with an X-ray mirror-camera (CM5-100, Canon Inc., Tokyo, Japan). The technical parameters consisted of tube voltage of 130 kV with adjustment of mAs by photo-timer, and a distance of 120 cm from the tube to film with a 2.0-mm aluminum filter. The film rolls were reviewed on dedicated illuminant miniature X-ray film viewers equipped with magnifying glasses. For screening with CT, images were obtained by mobile low-dose spiral CT equipment (W950SR, Hitachi Medical Co, Tokyo, tube voltage of 120 kV, electric current of 50 mA, rotation of $0.5\,s^{-1}$, collimation of 10 mm, interval of 10 mm). The images were reviewed on CRT with personal computer-based viewing and reporting system. Each image of X-ray and CT was reviewed by 2 independent expert pulmonologists, and any pulmonary or endobronchial nodule suggesting a lesion requiring further examinations was compared with a previous study when available. Then, the final judgment was given by several reviewers' consensual decision and the results were classified into 4 categories; no nodule (category I), nodules requiring no further examinations (category II), nodules suggesting non-malignant lesion requiring further examinations (including lesions suggesting active tuberculosis, category III), and nodules suggesting malignant lesions (category IV). There was no communication between X-ray and CT reviews. Further examinations consisted of conventional-dose CT with thin-section scanning, ranging from 0.5 to 2 mm thickness according to the requirement, in all patients with categories III and IV, follow-up studies by CT, and invasive diagnostic procedures including bronchoscopy, CT-guided biopsy and video-assisted thoracotomy when required.

The X-ray screening was repeated every year. Because of research resource limitation, the city was geographically divided into 2 areas, and the CT screening was performed alternatively in only one area each year, resulting in screening in the same area every 2 years. Inter-screening tracking of the subjects without categories III and IV was not allowed because of local regulations. Both screenings were performed from 2001 to 2004 in each fiscal year, with follow-up periods until September 2007. The entire study was approved by the Ethics Committee of the Chiba Foundation for Health Promotion & Disease Prevention.

2.3. Image analysis of detected lung cancer

Thin-section images of detected nodules definitively diagnosed as primary lung cancer were retrospectively reviewed and classified into 3 categories; pure ground glass attenuation (GGA), part solid (GGA with a central solid part) and solid nodule [15,16].

2.4. Statistics

Comparisons of frequency were performed by Student's t-test, and survival curves were drawn by Kaplan–Meier's method followed by comparison with log rank test. Differences with p values of less than 0.05 (two tailed) were judged as statistically significant.

3. Results

The total numbers of person-years for X-ray and CT screening in the 4-year period were 22,720 and 3305, with actual subject numbers of 8246 and 2550, respectively. Characteristics of the subjects are summarized in Table 1. In this

Table 1 Characteristics of subjects

Year	Total no. of subjects	Age (years)[a]	Sex		No. of baseline study	No. of repeat study
			No. of male (median age; range)	No. of female (median age, range)		
X-ray screening						
2001	5,309	59 (40–93)	1776 (63; 40–85)	3,533 (57; 40–93)	101	5,208
2002	5,417	58 (40–89)	1828 (62; 40–86)	3,589 (56; 40–89)	927	4,490
2003	5,782	59 (40–92)	2018 (63; 40–88)	3,764 (57; 40–92)	848	4,934
2004	6,212	60 (40–94)	2167 (63; 40–91)	4,045 (58; 40–94)	794	5,418
Total	22,720*	59 (40–94)	7789 (63; 40–91)	14,931 (57; 40–94)	2670	20,050*
CT screening						
2001 (area A)	729	65 (50–87)	326 (65; 50–85)	403 (66; 50–87)	729	NA
2002 (area B)	762	65 (50–84)	314 (66; 50–84)	448 (64; 50–81)	762	NA
2003 (area A)	838	65 (50–85)	361 (65; 50–83)	477 (64; 50–85)	519	319
2004 (area B)	976	65 (50–83)	419 (65; 50–83)	557 (64; 50–80)	540	436
Total	3,305*	65 (50–87)	1420 (65; 50–85)	1,885 (65; 50–87)	2550	755

[a] Median (range).
* Numbers in terms of person-years.

table, the actual number for CT screening is equal to the total number of subjects who participated in the baseline study because the screening was started at 2001. However, in the X-ray screening, the number of subjects participated in the repeat study at 2001 ($n=5208$) plus total number of subjects participated in the baseline study ($n=2670$) dose not result in the actual total number ($n=8246$) in 4 years, because the screening had been started before 2001; there were some subjects who had participated in the screening before 2001 and did not at 2001. In addition, the subject number of repeat study is greatly exceeds the number of baseline study in every year, because many subjects had already participated in the screening before 2001. Smoking status of the subjects is summarized in Fig. 1 according to gender and screening method. The subjects of CT screening consisted of a significantly higher proportion of smokers than those of X-ray screening ($p<0.001$ for males, and $p=0.0014$ for females, χ^2 test). Total accrual numbers of further examinations (categories III and IV) were 313 (78 category III and 235 category IV) of 22,720 (1.4%) in X-ray screening, and 337 (67 category III and 270 category IV) of 3305 (10.2%) in CT screening.

All lung cancers were found exclusively from category IV in both screenings. Lung cancers were found in 10 patients (0.044% of the 22,720 screened) through the X-ray screening, 4 patients by baseline (0.1498%, or 4 out of 2670) and 6 patients by repeat screening (0.030%, 6 out of 20,050). Among them, 5 (50%) patients had stage IA lung cancer. With CT screening, 15 patients (0.454% of the 3305 screened) with primary lung cancer were found. They were exclusively found in baseline screening, and all 15 lung cancers were stage IA. Patient characteristics are summarized in Table 2. With X-ray screening, lung cancer was detected in 0.040% (6/14,931) of female participants, and in 0.051% (4/7789) of male participants, with a female-to-male ratio of the detection rate of 0.78. In contrast, with CT screening, it was detected in 0.58% (11/1885) of female, and in 0.28% (4/1420) of male participants, with a female-to-male ratio of 2.07. The proportion of adenocarcinoma was 86.7% (13/15) in patients detected through CT screening, significantly higher than that (50%, or 5/10) in patients detected through X-ray screening ($p=0.0455$, χ^2 test). The constitution of the image type of lesions, that is, pure GGA, part solid and solid types, was significantly different between these 2 groups ($p=0.0001$, χ^2 test), and those detected by CT screening were more likely to be pure GGA or part solid than those detected by X-ray screening. Standard lobectomy with hilar and mediastinal lymph node dissection was performed in 6 of the 10 lung cancer patients detected by X-ray and in 14 of the 15 patients detected by CT screening (Table 2). Retrospective re-review of X-rays of patients with CT screening-detected lung cancer disclosed that the corresponding lesion was visible on X-ray in only one case, #CT-12.

Survival curves of the patients with detected lung cancer are shown in Fig. 2. Survival of the patients detected by CT screening was better than that of the patients detected by X-ray screening with statistical significance (Fig. 2A). Survival of the patients undergoing surgery was also compared between the patient groups detected by CT and X-ray screenings, again disclosing better survival in the CT screened patients than in the X-ray-detected patients with

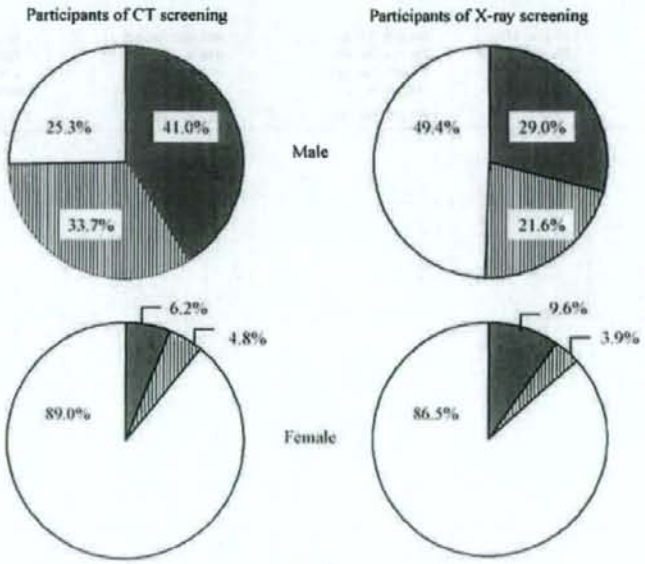

Fig. 1 Smoking status of the participants in the 2 screening programs. Closed, shaded and open areas represent current, ex- and never smokers, respectively. Smoking rates of the participants in the X-ray screening were similar to the general statistics in Japan, in both male and female populations, whereas those of the participants, especially in males, in the CT screening were significantly higher than in participants of the X-ray screening ($p<0.001$ for males, and $p=0.0014$ for females, χ^2 test), very possibly because of smokers' motivation to participate in CT screening.

Table 2 Characteristics of detected lung cancer

Case no.	Age	Sex	Size (mm)	Histology	Stage	Image type	Treatment	Visible on X-ray
With X-ray screening								
X-1	75	F	30[a]	Ad	p-IA	Solid	S[b]	NA
X-2	75	M	28	Sm	p-IB[c]	Solid	S and C	NA
X-3	70	F	20	Ad	p-IA	Solid	S	NA
X-4	77	M	50	Sq	c-IIIA	Solid	R	NA
X-5	74	M	20	Sq	c-IIIA	Solid	R	NA
X-6	78	F	8	Sm	c-IIIA	Solid	C and R	NA
X-7	51	F	25	Ad	p-IA	Solid	S	NA
X-8	47	M	27	Ad	c-IIIA	Solid	C and R	NA
X-9	69	F	10	Carcinoid	p-IA	Solid	S	NA
X-10	62	F	27	Ad	p-IA	Solid	S	NA
With CT screening								
CT-1	64	M	10	Ad	p-IA	Pure GGA	S	No
CT-2	72	F	11	Ad	p-IA	Pure GGA	S	No
CT-3	64	M	20	Ad	p-IA	Pure GGA	S	No
CT-4	63	F	15	Ad	p-IA	Part solid	S	No
CT-5	71	F	15	Ad	p-IA	Part solid	S	No
CT-6	79	M	14	Sq	p-IA	Solid	S	No
CT-7	66	F	7	Ad	p-IA	Pure GGA	S	No
CT-8	60	F	8	Ad	p-IA	Part solid	S	No
CT-9	67	F	15	Ad	p-IA	Part solid	S	No
CT-10	58	F	9	Ad	p-IA	Pure GGA	S	No
CT-11	63	F	10	Ad	p-IA	Pure GGA	S	No
CT-12[d]	59	M	23	Non-small	c-IA	Solid	BSC	Yes
CT-13	70	F	10	Ad	p-IA	Part solid	S	No
CT-14	62	F	10	Ad	p-IA	Part solid	S	No
CT-15	61	F	30	Ad	p-IA	Pure GGA	S	No

[a] Maximum diameter.
[b] S, R, C and BSC represent surgery, radiotherapy, chemotherapy and best supportive care, respectively.
[c] Postoperative evaluation of the tumor size determined the stage of IB.
[d] This patient was diagnosed as having clinical stage IA non-small cell lung cancer not further specified together with concomitant advanced esophageal cancer by staging procedures.

statistical significance (Fig. 2B). Two patients, detected by X-ray screening were dead after surgery, both from lung cancer recurrence (case #X-2 and 10).

4. Discussion

The present lung cancer screenings recruited subjects not limited to a high-risk group. First, the X-ray screening program was provided for general residents in a certain city in Japan, and the next screening program with CT was offered to the participants of the X-ray program, while excluding subjects who were judged to require further examinations by the X-ray screening. Therefore, the present CT screening program was eventually a screening for roentgen-negative lung cancer. The present study was preliminary and had several shortcomings: (1) sample size was relatively small, (2) there were some deviations in characteristics of the subjects; the subjects of X-ray screening consisted of less smokers and younger population especially in female than the subjects of CT screening, (3) examination was repeated every 2 years in the CT screening program, and (4) no inter-screening follow-up for counting lung cancer occurrence and death was performed, resulting in a lack of estimation of the true frequency of lung cancer occurrence in the subjects during the study period. In particular, the primary issues being the small sample size and the deviations in subject characteristics ostensibly limit this study's ability to make definitive conclusion. This kind of study solely enables us to evaluate screening efficacy by comparing CT screening with X-ray screening in terms of the characteristics of the detected lung cancer.

CT screening detected lung cancer at a frequency of approximately 10 times that of X-ray screening, even though CT screening was provided for X-ray screening-negative subjects. In addition, all lung cancers detected by CT were at stage IA, whereas only 6 of 10 lung cancers detected by X-ray screening were at stage IA, consequently resulting in better survival in the former compared to the latter. Characteristics of the lung cancer detected through CT screening were significantly different from those through X-ray screening. First of all, all 15 lung cancers detected by CT were adenocarcinomas except for one with non-small cell lung cancer not further specified, whereas only 5 of 10 lung cancers detected by X-ray screening were adenocarcinomas, the latter ratio being similar to that of the general statistics in Japan. Secondly, the female-to-male ratio of the detection rate with CT screening (2.07) was substantially higher than that with

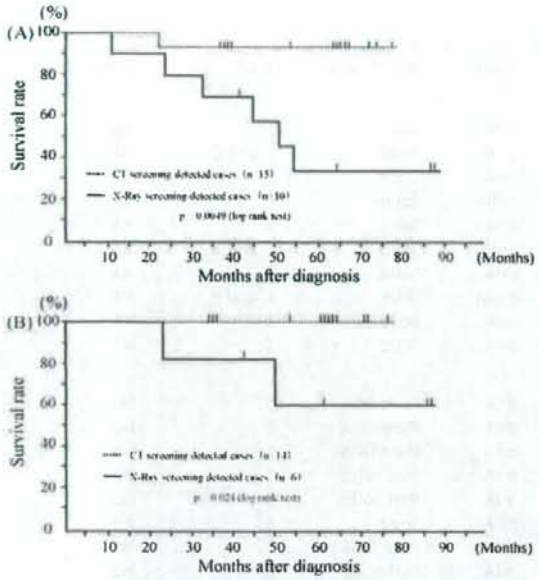

Fig. 2 Survival curves of patients with lung cancer according to screening method. Patients detected by CT screening ($n = 15$) survived significantly longer than patients detected by X-ray screening ($n = 10$, A). Comparison between the 2 groups limited to the subpopulations undergoing surgery showed a similar result (B). The curves were drawn by Kaplan–Meier's method, and compared with the log rank test.

X-ray screening (0.78). Considering that the female-to-male ratio of patients with lung cancer in the general statistics of Japan was 0.41 [17], the ratio with CT screening seemed extraordinarily high, and may actually be biased. As a matter of fact, the ratio with X-ray screening of 0.78 also seemed high, suggesting strong bias with screening. Thirdly, when assessed with thin-section CT, the image type of the lung cancer detected by CT screening contained a significantly larger portion of pure GGA or part solid type than that by X-ray screening. This is quite reasonable because nodules of GGA type are notoriously invisible on X-ray. The existence of GGA either as pure GGA or in part solid nodules in thin-section CT represents air-spaces in lung adenocarcinoma tissue, and very likely corresponds to either type A, B, or C of peripheral small adenocarcinoma [15,16,18–21] according to Noguchi's classification [22]. Such lung adenocarcinomas, in most cases, are characterized by a slow-growing nature and good prognosis with lung resection [15,16,18–22].

Effective cancer screening requires several conditions including the followings: (1) the screening is capable of detecting corresponding cancer at a high frequency, (2) prognosis of patients with screening-detected cancer is significantly better than that of patients found by symptoms, (3) less patients with advanced cancer and deaths from the cancer are shown by the screening, and (4) the screening is affordable in respect to human resource and cost. Many previous studies [5,11,13,23–27] and two recent studies [10,14] on lung cancer screening by CT provided evidence for the first 2 conditions. The present study also supports these previous study results. Bach et al., however, cast doubt on lower number of patients with advanced disease and lung cancer deaths by CT screening [14]. The discrepancy between the high frequency of early detection resulting in good prognosis of the detected patients and a lack of decrease in advanced disease and death may be partly explained by overdiagnosis through screening. That is to say, in spite of a definitive histological diagnosis, many early lung cancers detected through screening would not progress rapidly to the point of being clinically overt in the individual's lifetime. In fact, lung cancers detected via the present CT screening seemed to possess less malignant propensity, because the majority (13 out of 15 patients) were classified into either pure GGA or part solid type adenocarcinomas by thin-section CT findings, and because they were found predominantly in female non-smokers. In particular, detection and diagnosis in one patient (#CT-12) was apparently overdiagnosed because he died from concomitant advanced esophageal cancer while his lung cancer was at clinical stage IA. Nevertheless, the rest of the lung cancers detected by the present CT screening would have very possibly progressed to clinically overt and fatal cancer if left untreated, making it needless to refer in particular to the I-ELCAP study [10], in which 8 patients with clinical stage I cancer detected by CT screening did not receive treatment, with all of them dying within 5 years. In addition, any individual with pulmonary nodules judged to require further examinations through X-ray screening was excluded from enrollment to the CT screening. Most lung cancers detected by X-ray screening would have been detected by CT screening if no X-ray screening had been provided. Therefore, the present CT screening has the potential to reduce advanced lung cancer or death from lung cancer in the future, but not within a few years. Although Bach et al. failed to demonstrate a decrease in advanced disease and death from lung cancer [14], the reason for the negative result may be related to a relatively short median follow-up period of 3.9 years. Needless to say, large-scale randomized controlled studies that eliminate biases would have advantages for drawing definitive conclusions. Hence, results from randomized controlled studies such as the National Lung Screening Trial in the United States and the NELSON Trial in Europe are awaited [14,28,29]. It is important, however, to understand that a substantially long follow-up period, although difficult to be estimated from this study, would be required even in the case of well-sophisticated randomized controlled studies. Considerations on potential harm and cost would also be an important issue.

In conclusion, the present study confirmed the capability of CT screening in detecting early stage lung cancer at a high frequency, and suggested that CT screening-detected lung cancer might have less malignant propensity than X-ray screening-detected or symptom-detected lung cancer. In CT screening for lung cancer, a considerably extended follow-up period would be essential for evaluating its effectiveness in decreasing lung cancer mortality.

Conflict of interest

There exists no potential conflict of interest with regard to the manuscript in every author.

Acknowledgements

The authors thank Drs. Reiko Uruma, Jun-ichi Yasuda, Kazutoshi Sugito, Masato Shingyoji and Yoshiko Asaka-Amano for reviewing CT images. Technical and secretarial assistance by Mses. Naoko Oodaira (Chiba Foundation for Health Promotion & Disease Prevention), and Chieko Miyagi-Handa are also appreciated. Assistance in database management by Ms. Mariko Maru, PHN, is especially appreciated. This research was financially supported by grants to the Chiba Foundation for Health Promotion & Disease Prevention from Chiba Prefecture and by grants to YT from the Ministry of Education, Culture, Sports, Science and Technology of Japan.

References

[1] Fontana RS, Sanderson DR, Woolner LB, Taylor WF, Miller WE, Muhm JR, et al. Screening for lung cancer. A critique of the Mayo Lung Project. Cancer 1991;67:1155–64.

[2] Marcus PM, Bergstralh EJ, Fagerstrom RM, Williams DE, Fontana R, Taylor WF, et al. Lung cancer mortality in the Mayo Lung Project: impact of extended follow-up. J Natl Cancer Inst 2000;92:1308–16.

[3] Strauss GM. The Mayo Lung Cohort: a regression analysis focusing on lung cancer incidence and mortality. J Clin Oncol 2002;20:1973–83.

[4] Marcus PM, Bergstralh EJ, Zweig MH, Harris A, Offord KP, Fontana RS. Extended lung cancer incidence follow-up in the Mayo Lung Project and overdiagnosis. J Natl Cancer Inst 2006;98:748–56.

[5] Nawa T, Nakagawa T, Kusano S, Kawasaki Y, Sugawara Y, Nakata H. Lung cancer screening using low-dose spiral CT: results of baseline and 1-year follow-up studies. Chest 2002;122:15–20.

[6] Mountain CF. Revisions in the International System for Staging Lung Cancer. Chest 1997;111:1710–7.

[7] Diederich S, Wormanns D, Semik M, Thomas M, Lenzen H, Roos N, et al. Screening for early lung cancer with low-dose spiral CT: prevalence in 817 asymptomatic smokers. Radiology 2002;222:773–81.

[8] Sobue T, Moriyama N, Kaneko M, Kusumoto M, Kobayashi T, Tsuchiya R, et al. Screening for lung cancer with low-dose helical computed tomography: anti-lung cancer association project. J Clin Oncol 2002;20:911–20.

[9] Swensen SJ, Jett JR, Sloan JA, Midthun DE, Hartman TE, Sykes A-M, et al. Screening for lung cancer with low-dose spiral computed tomography. Am J Respir Crit Care Med 2002;165:508–13.

[10] The International Early Lung Cancer Action Program I. Survival of patients with stage I lung cancer detected on CT screening. N Engl J Med 2006;355:1763–71.

[11] Henschke CI, McCauley DI, Yankelevitz DF, Naidich DP, McGuinness G, Miettinen OS, et al. Early Lung Cancer Action Project: overall design and findings from baseline screening. Lancet 1999;354:99–105.

[12] Sone S, Li F, Yang ZG, Honda T, Maruyama Y, Takashima S, et al. Results of three-year mass screening programme for lung cancer using mobile low-dose spiral computed tomography scanner. Br J Cancer 2001;84:25–32.

[13] Sone S, Nakayama T, Honda T, Tsushima K, Li F, Haniuda M, et al. Long-term follow-up study of a population-based 1996-1998 mass screening program for lung cancer using mobile low-dose spiral computed tomography. Lung Cancer 2007;58:329–41.

[14] Bach PB, Jett JR, Pastorino U, Tockman MS, Swensen SJ, Begg CB. Computed tomography screening and lung cancer outcomes. JAMA 2007;297:953–61.

[15] Aoki T, Nakata H, Watanabe H, Nakamura K, Kasai T, Hashimoto H, et al. Evolution of peripheral lung adenocarcinomas: CT findings correlated with histology and tumor doubling time. Am J Roentgenol 2000;174:763–8.

[16] Hasegawa M, Sone S, Takashima S, Li F, Yang ZG, Maruyama Y, et al. Growth rate of small lung cancers detected on mass CT screening. Br J Radiol 2000;73:1252–9.

[17] Cancer Statistics in Japan—2007. Tokyo, Japan: Foundation for Promotion of Cancer Research; 2007. p. 68–75.

[18] Jang HJ, Lee KS, Kwon OJ, Rhee CH, Shim YM, Han J. Bronchioloalveolar carcinoma: focal area of ground-glass attenuation at thin-section CT as an early sign. Radiology 1996;199:485–8.

[19] Aoki T, Tomoda Y, Watanabe H, Nakata H, Kasai T, Hashimoto H, et al. Peripheral lung adenocarcinoma: correlation of thin-section CT findings with histologic prognostic factors and survival. Radiology 2001;220:803–9.

[20] Kodama K, Higashiyama M, Yokouchi H, Takami K, Kuriyama K, Mano M, et al. Prognostic value of ground-glass opacity found in small lung adenocarcinoma on high-resolution CT scanning. Lung Cancer 2001;33:17–25.

[21] Yang Z-G, Sone S, Takashima S, Li F, Honda T, Maruyama Y, et al. High-resolution CT analysis of small peripheral lung adenocarcinomas revealed on screening helical CT. Am J Roentgenol 2001;176:1399–407.

[22] Noguchi M, Morikawa A, Kawasaki M, Matsuno Y, Yamada T, Hirohashi S, et al. Small adenocarcinoma of the lung. Histologic characteristics and prognosis. Cancer 1995;75:2844–52.

[23] Kaneko M, Eguchi K, Ohmatsu H, Kakinuma R, Naruke T, Suemasu K, et al. Peripheral lung cancer: screening and detection with low-dose spiral CT versus radiography. Radiology 1996;201:798–802.

[24] Sone S, Takashima S, Li F, Yang Z, Honda T, Maruyama Y, et al. Mass screening for lung cancer with mobile spiral computed tomography scanner. Lancet 1998;351:1242–5.

[25] Henschke CI, Naidich DP, Yankelevitz DF, McGuinness G, McCauley DI, Smith JP, et al. Early lung cancer action project: initial findings on repeat screenings. Cancer 2001;92:153–9.

[26] Swensen SJ, Jett JR, Hartman TE, Midthun DE, Mandrekar SJ, Hillman SL, et al. CT screening for lung cancer: five-year prospective experience. Radiology 2005;235:259–65.

[27] Swensen SJ, Jett JR, Hartman TE, Midthun DE, Sloan JA, Sykes AM, et al. Lung cancer screening with CT: Mayo Clinic experience. Radiology 2003;226:756–61.

[28] Black WC, Baron JA. CT screening for lung cancer: spiraling into confusion? JAMA 2007;297:995–7.

[29] Twombly R. Lung cancer screening debate continues despite international CT study results. J Natl Cancer Inst 2007;99:190–5.

the FEBS Journal

Mitogen-activated protein kinase phosphatase-1 modulated JNK activation is critical for apoptosis induced by inhibitor of epidermal growth factor receptor-tyrosine kinase

Kenji Takeuchi[1], Tomohiro Shin-ya[1], Kazuto Nishio[2] and Fumiaki Ito[1]

1 Department of Biochemistry, Faculty of Pharmaceutical Sciences, Setsunan University, Osaka, Japan
2 Department of Genome Biology, Kinki University School of Medicine, Osaka, Japan

Keywords
AG1478; c-Jun N-terminal kinase; epidermal growth factor receptor; mitogen-activated protein kinase phosphatase-1; non-small-cell lung cancer

Correspondence
K. Takeuchi, Department of Biochemistry, Faculty of Pharmaceutical Sciences, Setsunan University, Hirakata, Osaka 573-0101, Japan
Fax: +81 72 866 3117
Tel: +81 72 866 3118
E-mail: takeuchi@pharm.setsunan.ac.jp

(Received 29 August 2008, revised 6 December 2008, accepted 16 December 2008)

doi:10.1111/j.1742-4658.2008.06861.x

Alterations resulting in enhanced epidermal growth factor receptor (EGFR) expression or function have been documented in a variety of tumors. Therefore, EGFR-tyrosine kinase is a promising therapeutic target. Although *in vitro* and *in vivo* studies have shown the anti-tumor activity of EGFR-tyrosine kinase inhibitors against various tumor types, little is known about the mechanism by which such inhibitors effect their anti-tumor action. AG1478 is known to selectively inhibit EGFR-tyrosine kinase. In this study, we showed that AG1478 caused apoptosis and apoptosis-related reactions such as the activation of caspase 3 in human non-small cell lung cancer cell line PC-9. To investigate the signaling route by which AG1478 induced apoptosis, we examined the activation of c-Jun N-terminal kinase (JNK) and mitogen-activated protein kinase p38 in AG1478-treated PC-9 cells. JNK, but not p38, was significantly activated by AG1478 as determined by both immunoblot analysis for levels of phosphorylated JNK and an *in vitro* activity assay. Various types of stimuli activated JNK through phosphorylation by the dual-specificity JNK kinases, but the dual-specificity JNK kinases MKK4 and MKK7 were not activated by AG1478 treatment. However, JNK phosphatase, i.e. mitogen-activated protein kinase phosphatase-1 (MKP-1), was constitutively expressed in the PC-9 cells, and its expression level was reduced by AG1478. The inhibition of JNK activation by ectopic expression of MKP-1 or a dominant-negative form of JNK strongly suppressed AG1478-induced apoptosis. These results reveal that JNK, which is activated through the decrease in the MKP-1 level, is critical for EGFR-tyrosine kinase inhibitor-induced apoptosis.

Epidermal growth factor receptor (EGFR), a member of the ErbB family, is important in the regulation of growth, differentiation and survival of various cell types. Ligand binding to EGFR results in receptor dimerization, activation of its tyrosine kinase and phosphorylation of its C-terminal tyrosine residues. The tyrosine-phosphorylated motifs of EGFR recruit various adaptors or signaling molecules [1,2]. EGFR is able to activate a variety of signaling pathways through its association with these molecules. The mitogen-activated protein kinase (MAPK) pathway leading to phosphorylation of extracellular signal-regulated

Abbreviations
EGFR, epidermal growth factor receptor; ERK, extracellular signal-regulated kinase; JNK, c-Jun N-terminal kinase; MAPK, mitogen-activated protein kinase; MKP-1, mitogen-activated protein kinase phosphatase-1; NSCLC, non-small-cell lung cancer; PI, propidium iodide; PtdIns3-K, phosphatidylinositol 3-kinase; SAPK, stress-activated MAPK

kinase (ERK) 1/2 plays an essential role in EGF-induced cell growth; and the phosphatidylinositol 3-kinase (PtdIns3K) pathway is also important for cell growth and cell survival. One way by which PtdIns3K signals cells to survive is by activating protein kinase PDK1 which in turn phosphorylates Akt.

EGFR gene mutations or EGFR gene amplification is detected in various types of malignancy [1,2]; therefore, EGFR-tyrosine kinase is a promising therapeutic target. Orally active small molecules against EGFR (e.g. gefitinib and erlotinib) show evident anti-tumor effects in patients with various cancers, particularly non-small cell lung cancer (NSCLC) [3–5]. Beneficial responsiveness to EGFR-targeting chemicals in NSCLC patients is closely associated with EGFR mutations in the kinase domain [6–8].

The induction of apoptosis has been considered as a major mechanism for gefitinib-mediated anti-cancer effects [9,10]. Lung cancer cells harboring mutant EGFRs become dependent on them for their survival and, consequently, undergo apoptosis following inhibition of EGFR tyrosine kinase by gefitinib. Gefitinib has been shown to inhibit cell survival and growth signaling pathways such as the Ras-MAPK pathway and PtdIns3K/Akt pathway, as a consequence of inactivation of EGFR [10–13]. The PtdIns3K/Akt pathway is downregulated in response to gefitinib only in NSCLC cell lines that are growth-inhibited by gefitinib [14]. So, it is thought that the PtdIns3K/Akt pathway plays a critical role in the gefitinib-induced anti-tumor action. Furthermore, some reports have demonstrated that blockage of the EGFR activity with gefitinib is able to cause suppression of a downstream signaling pathway through Ras-MAPK and/or PtdIns3K/Akt, and induce apoptosis through activation of the pro-apoptotic Bcl-2 family protein Bad or Bax [9,15].

In mammals, three major groups of MAPK have been identified [16–18]. The c-Jun N-terminal kinase (JNK), also known as stress-activated MAPK (SAPK), represents a group of MAPKs that are activated by treatment of cells with cytokines or by exposure of cells to a variety of stresses [19–21]. JNK activity has been implicated in both apoptosis and survival signaling and is tightly controlled by both protein kinases and protein phosphatases [22–24]. Various types of stimuli activate JNK through phosphorylation by the dual-specificity kinase MKK4 or MKK7 [18,25]. By contrast, any types of stimuli can inactivate JNK through induction of the expression of JNK phosphatases, which include dual-specificity (threonine/tyrosine) phosphatases [26–28].

PC-9 cells are gefitinib-sensitive human NSCLC cell lines with a mutation (delE746-A750) in their EGFR, which allows the receptor to be autophosphorylated independent of EGF. In this study, we investigated the signaling route by which the EGFR tyrosine kinase inhibitor AG1478 induces apoptosis in PC-9 cells. There is a general agreement on the hypothesis that the inhibition of ERK1/2 MAPK and/or PtdIns3K/Akt growth/survival signaling cascades leads to apoptosis of cancer cells. However, there are no studies addressing the role of JNK in apoptosis induced by EGFR tyrosine kinase inhibitors. Here, we demonstrate that JNK-phosphatase MKP-1 expression is controlled by a signal downstream of EGFR and that if this signal is abolished by an inhibitor of EGFR tyrosine kinase, the decreased MKP-1 activity can result in JNK activation, leading to the induction of apoptosis.

Results

We first examined the effect of AG1478 on the viability of human NSCLC cell line PC-9. Treatment of the cells with AG1478 markedly suppressed the cell viability, as determined by the results of a colorimetric assay (Fig. 1A). Photographic observation of AG1478-treated PC-9 cells revealed that AG1478 decreased the percentage of adherent cells in a time-dependent manner (Fig. 1B). When AG1478-treated PC-9 cells were stained with Hoechst–propidium iodide (PI), cells with condensed chromatin and fragmented nuclei, which are characteristic of the nuclear changes in apoptotic cells, were seen in both adherent and non-adherent cell populations (data not shown). To confirm whether this AG1478-induced cell death resulted from apoptosis, we examined caspase 3 activity after exposing the cells to 500 nM AG1478. As shown in Fig. 1C, caspase 3 activity was increased in a time-dependent manner. It thus appears that AG1478 reduced the survival rate of PC-9 cells by activating the apoptotic pathway.

It is important to know how AG1478 affected the survival rate of PC-9 cells. Many studies have shown that enhanced JNK activity may be required for initiation of stress-induced apoptosis [29,30]. To examine whether JNK might be activated by AG1478, we treated PC-9 cells with AG1478 for various periods (Fig. 2A). Activation of JNK was measured by performing an immune complex kinase assay using bacterially expressed GST–c-Jun as a substrate. Phosphorylation of c-Jun appeared 1 h after AG1478 addition, with a maximum level at 24 h. We next determined the phosphorylation of JNK in the presence of AG1478. PC-9 cells were incubated with AG1478 for several periods, and cell lysates were prepared from these cells to determine the phosphorylation of JNK by immunoblotting (Fig. 2B). AG1478

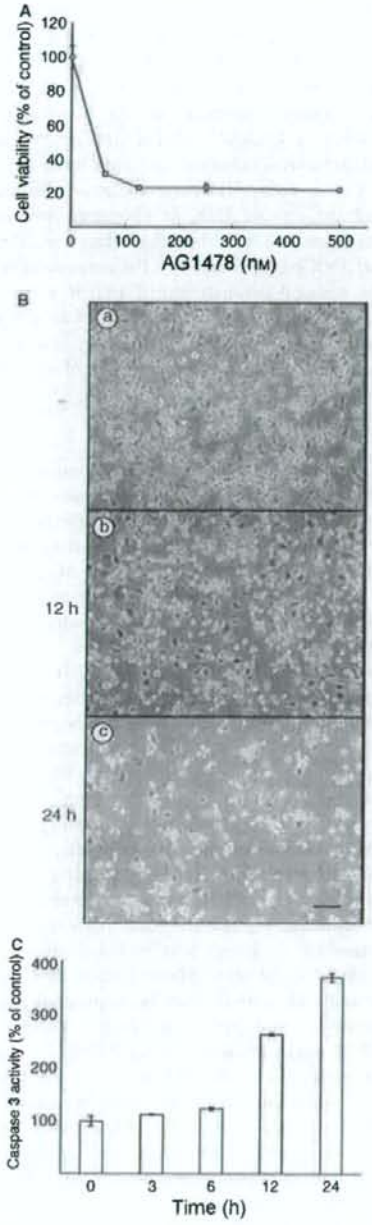

Fig. 1. Induction of apoptosis by AG1478. (A) PC-9 cells were seeded into a 96-well microplate, and treated with AG1478 at various concentrations for 48 h. The viability of cells was determined by conducting WST-8 assays. The value of untreated cells was considered as 100% viability. The data presented are the mean ± SD ($n = 6$). (B) PC-9 cells were seeded at a density 3×10^5 cells per 60 mm dish and then treated with 500 nM AG1478. The phase-contrast photomicrographs were taken 0 (a), 12 (b) or 24 h (c) after incubation with AG1478. Scale bar, 100 μm. (C) PC-9 cells were treated with 500 nM AG1478. Lysates were prepared at the indicated time points after the AG1478 addition and analyzed for caspase **3** activity by using a fluorometric substrate-based assay. Each point is the mean of triplicate samples, and the bar represents the standard deviation. Similar results were obtained from three separate experiments.

Fig. 2. JNK activation by AG1478. PC-9 cells were treated with 500 nM AG1478 and lysed on ice at the indicated time points. (A) JNK–c-Jun complexes were collected by glutathione *S*-transferase–c-Jun agarose beads and then assayed *in vitro* for kinase activity by using c-Jun as a substrate. The phospho-c-Jun product was detected by immunoblotting. (B) The cell lysates were normalized for protein content and analyzed for phospho-JNK content (upper), as well as for JNK content (lower). (C) The cell lysates were analyzed for phospho-p38 content (upper panel), as well as for p38 (lower). Similar results were obtained from three separate experiments.

intensively stimulated phosphorylation of JNK on its threonine 183 and tyrosine 185, and their phosphorylation levels continued to increase for at least 24 h. However, the activation of p38, another MAP kinase sub-family member, was not evident up to 12 h after AG1478 treatment; although an increase in the phosphorylation of p38 was detected at 24 h (Fig. 2C). Phosphorylation of ERK1/2, prototypical MAPK, was decreased by the treatment with AG1478 at the same time as activation of JNK (data not shown).

Neither SB203580 nor PD98059, inhibitors of p38 and ERK1/2, respectively, affected AG1478-induced apoptosis in PC-9 cells (data not shown), suggesting that neither p38 nor ERK1/2 mainly transmit the apoptotic signal of AG1478 in the PC-9 cells. If JNK plays an important role in AG1478-induced apoptosis,

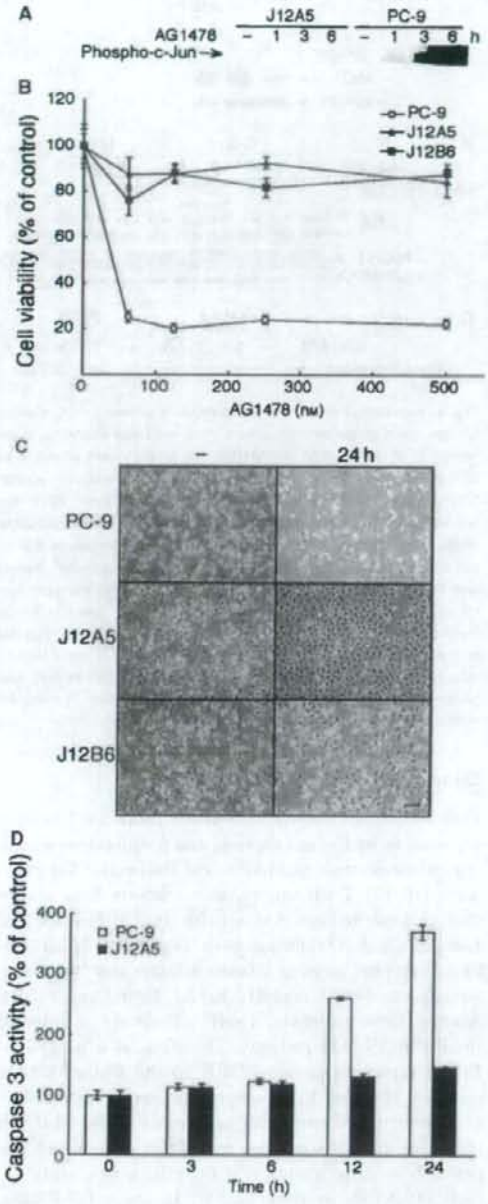

Fig. 3. Expression of dominant-negative JNK prevents AG1478-induced apoptosis. (A) Subconfluent PC-9 and J12A5 cells were incubated with 500 nM AG1478 for the indicated times. JNK activity was determined as described in Experimental Procedures. (B) PC-9, J12A5 and J12B6 cells were incubated with the indicated concentrations of AG1478 for 48 h. The viability of cells was determined by conducting WST-8 assays. The reading obtained for untreated cells was considered as 100% viability. The data presented are the mean ± SD ($n = 6$). (C) Phase-contrast photomicrographs were taken 24 h after incubation with 500 nM AG1478. Scale bar, 100 μm. (D) PC-9 and J12A5 cells were treated with 500 nM AG1478. Lysates were prepared at the indicated time points after the AG1478 addition and analyzed for caspase **3** activity by using a fluorometric substrate-based assay. Each point is the mean of the triplicate samples, and the bar represents the standard deviation. Similar results were obtained from three separate experiments.

inactivation of JNK should suppress this AG1478-induced apoptosis. To test this scenario, we stably transfected PC-9 cells with a mammalian expression vector encoding a dominant-negative form of JNK, and isolated two clones, J12A5 and J12B6. The results of a JNK kinase assay confirmed that J12A5 cells had no detectable activity (Fig. 3A). A colorimetric assay for cell viability, microscopic observation of cells, and an assay for caspase **3** activity revealed that this dominant-negative kinase efficiently blocked AG1478-induced apoptosis (Fig. 3B–D), indicating that activation of JNK mediated the AG1478-induced apoptosis.

A multitude of stimuli including osmotic stress activate JNK through phosphorylation of the JNK kinases MKK4 and MKK7 [18,31]. To examine the mechanism by which AG1478 induced JNK activation, we incubated PC-9 cells in the presence of AG1478 for several periods, and then prepared cell lysates from these cells to determine the phosphorylation of MKK4 and MKK7 by immunoblotting (Fig. 4A). No phosphorylated MKK4 or MKK7 was observed in the presence of AG1478, although phosphorylation of both JNK kinases in response to osmotic stress could be detected. Next, we determined the effect of AG1478 on the levels of MAPK phosphatases MKP-1 and MKP-2. As shown in Fig. 4B, AG1478 decreased the expression of the MKP-1 protein. As for the MKP-2 protein, however, AG1478 did not affect its expression level.

To check the role of MKP-1 as an anti-apoptotic signal molecule, we constitutively expressed MKP-1 in PC-9 cells. The cells were transfected with a vector directing the expression of MKP-1; and two clones, M1A4 and M1B2, were isolated as cell lines over-expressing MKP-1 (Fig. 5A). Using PC-9 and M1A4 cells, we examined the effect of AG1478 on the amounts of dually phosphorylated JNK (Fig. 5B). In PC-9 cells, AG1478 treatment decreased the expression of the MKP-1 protein and concomitantly stimulated the phosphorylation of JNK. However, the expression

Fig. 4. Effect of AG1478 on phosphorylation of MKK4 and MKK7, and expression of MKP-1 and MKP-2. A, PC-9 cells were treated with 500 nM AG1478 for the indicated periods, and cellular lysates were analyzed by SDS/PAGE and immunoblotting with anti-[phospho SEK1/MKK4 (Ser264/Thr261)] Ig and anti-[phospho MKK7 (Ser271/Thr275)] Ig, respectively (upper). α-Tubulin levels were examined as a control for equal loading (lower). As a control for MKK4 and MKK7 activation, parallel cultures were treated with 0.5 M sorbitol for 30 min or with 0.5 M sodium chloride for 15 min. (B) The cellular lysates were prepared at the indicated time points after AG1478 treatment. Total protein (40 μg) was subjected to immunoblotting, and the membranes were hybridized with antibodies against MKP-1 (upper) or MKP-2 (middle). The equal loading of the samples was checked by using an antibody against α-tubulin (lower). The experiments corresponding to (A) and (B) were repeated three times with similar results.

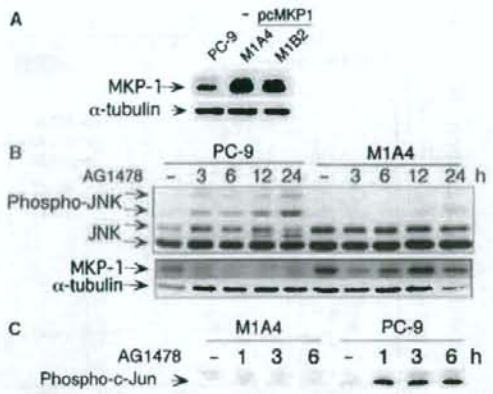

Fig. 5. Expression of MKP-1 prevents JNK activation. (A) Cellular lysates were prepared from parent PC-9 cells and pcMKP1- transfected PC-9 cells (M1A4 and M1B2). The lysates were analyzed by SDS/PAGE and immunoblotting with specific antibody against MKP-1 (upper) or α-tubulin (lower). (B) Subconfluent PC-9 and M1A4 cells were incubated with 500 nM AG1478 for the indicated times. The cells were then harvested, and equal aliquots of protein extracts (40 μg per lane) were analyzed for phospho-JNK (upper) and MKP-1 (lower) by immunoblotting. Each membrane was reprobed with JNK (upper) or an α-tubulin antibody (lower). Similar results were obtained from three separate experiments. (C) Cell lysates were prepared from PC-9 and M1A4 cells at the indicated time points after treatment with 500 nM AG1478. JNK activity was determined as described in Experimental procedures. The experiments were repeated three times with similar results.

level of MKP-1 in M1A4 cells remained high, in contrast to that in PC-9 cells; although MKP-1 expression was lowered once at 3 h after AG1478 treatment. JNK phosphorylation was extremely low in M1A4 cells. The expression patterns of MKP-1 and phospho-JNK seen in M1A4 were also observed in M1B2 cells (data not shown). The results of the JNK kinase assay indicated that JNK was not activated in M1A4 cells, where the MKP-1 expression level remained high even after exposure to AG1478 (Fig. 5C).

We next tested whether the expression level of MKP-1 correlated with sensitivity to AG1478. As shown in Fig. 6A,B, overexpression of MKP-1 resulted in resistance to AG1478. We also examined whether AG1478 could activate the effector caspase 3 in M1A4 cells (Fig. 6C). In PC-9 cells, activation of caspase 3 was observed with a maximal increase (480%) at 24 h after AG1478 treatment; however, in M1A4 cells, only a slight increase in caspase 3 enzyme activity (28% and 39% at 12 and 24 h, respectively) was detected. These results show that the MKP-1 expression level correlated with the susceptibility to AG1478-induced apoptosis.

Discussion

Gefitinib, an EGFR-tyrosine kinase inhibitor, has been reported to inhibit cell survival and proliferation signaling pathways such as MAPK and PtdIns3K/Akt pathways [10-13]. Furthermore, some reports have shown that gefitinib reduces Akt activity only in NSCLC cell lines, in which it inhibits growth [14,32]. The ErbB family of receptor tyrosine kinases includes four members, namely, the EGFR (ErbB1), ErbB2, ErbB3 and ErbB4. Among these members, ErbB3 effectively couples to the PtdIns3K/Akt pathway. Therefore, it is likely that ErbB3 serves to couple EGFR to the PtdIns3K/Akt pathway and that ErbB3 expression serves as an effective predictor of sensitivity to gefitinib in NSCLC cell lines [14]. In this study, we used PC-9 cells, which are gefitinib-sensitive human NSCLC cells with a mutation (delE746-A750) in their EGFR. In these PC-9 cells, autophosphorylation of EGFR took place independent of EGF, and it was suppressed by AG1478. Because AG1478 inhibited the phosphorylation of multiple down-stream targets including ERK1/2 in the PC-9 cells, but its effect on Akt phosphorylation was not so

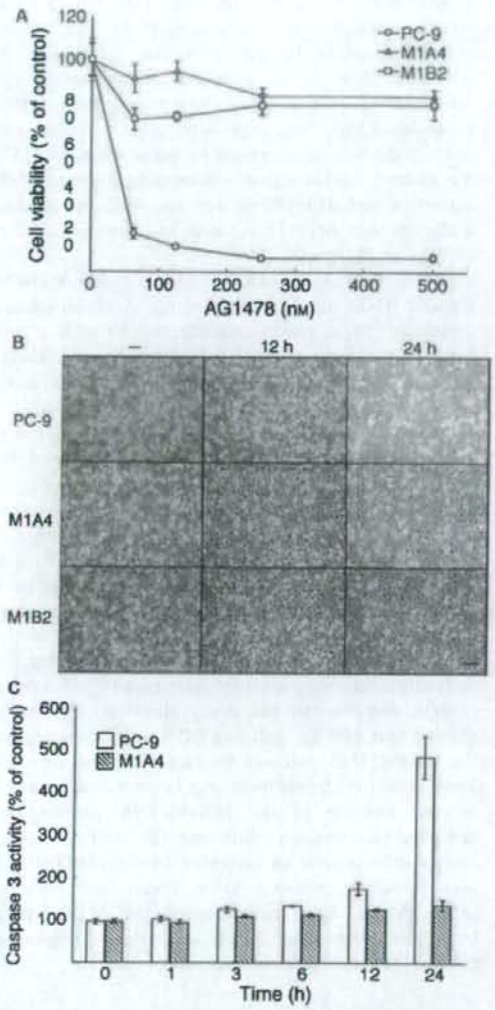

Fig. 6. Expression of MKP-1 prevents AG1478-induced apoptosis. A, PC-9, M1A4, and M1B2 cells were incubated with the indicated concentrations of AG1478 for 48 h. The viability of cells was determined by conducting WST-8 assays. The reading obtained for untreated cells was considered as 100% viability. The data presented are the mean ± SD ($n = 6$). (B) Phase-contrast photomicrographs were taken 12 and 24 h after incubation with 500 nM AG1478. Scale bar, 100 μm. (C) PC-9 and M1A4 cells were treated with 500 nM AG1478. Lysates were prepared at the indicated time points after the AG1478 addition and analyzed for caspase 3 activity by using a fluorometric substrate-based assay. Each point is the mean of the triplicate samples, and the bar represents the standard deviation. Similar results were obtained from three separate experiments.

significant (K. Takeuchi & F. Ito, unpublished data), intracellular signaling pathways other than PtdIns3K/Akt could be responsible for the AG1478-induced apoptosis in PC-9 cells.

Stress stimuli that induce apoptosis, including UV- and γ-irradiation, heat shock, protein synthesis inhibitors, DNA-damaging agents and the proinflammatory cytokines, are potent activators of JNK. Several anti-neoplastic agents such as cisplatin, etoposide, camptothecin and taxol, which are also strong inducers of apoptosis, also activate the JNK pathway [33]. In this study, we found that AG1478 induced the activation of JNK in PC-9 cells. Furthermore, a dominant-negative form of JNK efficiently blocked AG1478-induced apoptosis. It thus appears that EGFR-tyrosine kinase inhibitors induce apoptosis in PC-9 cells via activation of JNK.

ERK1 and ERK2, also known as p44 and p42 MAPK, respectively, represent the prototypical MAPK in mammalian cells. ERK MAP kinase catalytic activation was observed in PC-9 cells, and it was inhibited by AG1478. Increased phosphorylation of the other MAPK family member, p38, was also observed at 24 h after AG1478 treatment; but it was not observed at 12 h when apoptosis could be detected (Figs 1A and 2C). Our experiment indicated that neither SB203580 nor PD98059, inhibitors of p38 and ERK1/2, respectively, affected AG1478-induced apoptosis in PC-9 cells. Taken together, our data indicate that JNK, but not other MAPK family members such as p38 and ERK1/2, mainly transmits the apoptotic signal of AG1478 in the PC-9 cells.

JNK signaling can regulate apoptosis both positively and negatively, depending on the cell type, cellular context and the nature and dose of treatment [22,23]. Strong and sustained JNK activation is predominantly associated with induction or enhancement of apoptosis, whereas transient JNK activation can result in cell survival [23,24]. AG1478 induced strong and sustained JNK activation in PC-9 cells (Fig. 2A,B). This finding strengthens the possibility that JNK is a mediator of the apoptotic action of AG1478.

JNK activity in cells is tightly controlled by both protein kinases such as MKK4 or MKK7 and protein phosphatases such as MKPs. MKP-1, the first member of the MKP family to be identified as an ERK-specific phosphatase, is also able to inactivate JNK and p38 [34–38]. MKP-1 is an immediate-early gene whose expression is regulated by mitogenic, inflammatory and DNA-damaging stimuli [39–41]. In this study, we observed no activation of MKK4 or MKK7 in AG1478-treated PC-9 cells (Fig. 4A). However, the expression level of MKP-1, but not that of MKP-2,

was significantly decreased by the AG1478 treatment (Fig. 4B), indicating that JNK activity in the PC-9 cells may be regulated by MKP-1. Another member of the dual-phosphatase family of proteins, MKP-2 shows a 60% sequence homology to MKP-1, and also similar substrate specificity [42]. However, the expression level of MKP-2 was not affected by AG1478 treatment, indicating that the expression of MKP-1, but not that of MKP-2, is controlled by signals via EGFRs.

Brondello *et al.* reported that activation of the ERK cascade is sufficient to promote the expression of MKP-1 and MKP-2 [43]. It has also been suggested that MKP-1 expression is regulated by ERK-dependent and -independent signals [44]. Because the ERK inhibitor PD98059 did not affect MKP-1 expression or activation of JNK in PC-9 cells (K. Takeuchi & F. Ito, unpublished data), MPK-1 expression in PC-9 cells may be controlled in an ERK-independent manner. Recently, Ryser *et al.* reported that MKP-1 transcription is regulated in the transcriptional elongation step: under basal conditions, a strong block to elongation in the first exon regulates MKP-1 gene transcription [45]. Thus, EGFR-mediated signals may overcome this block to stimulate MKP-1 gene transcription in PC-9 cells. Another possible mechanism responsible for EGFR-mediated enhancement of MKP-1 expression is that MKP-1 degradation via the ubiquitin–proteasome pathway is suppressed by EGFR activation. In fact, some research groups have reported that the expression level of MKP-1 is controlled via the ubiquitin–proteasome pathway [46,47]. Our preliminary experiment also indicated that AG1478-induced MKP-1 degradation was suppressed in the presence of proteasome inhibitors such as MG-132 and ALLN (K. Takeuchi & F. Ito, unpublished data).

Gene disruption studies demonstrate that JNK is required for the release of mitochondrial proapoptotic molecules (including cytochrome *c*) and apoptosis in response to UV radiation [48]. Bax and Bak (members of the proapoptotic group of multidomain Bcl-2-related proteins) are essential for the JNK-stimulated release of cytochrome *c* and apoptosis [49]. Other studies have shown that 14-3-3 proteins are direct targets of JNK and that phosphorylation of 14-3-3 proteins by JNK results in dissociation of Bax from 14-3-3 proteins, leading to apoptosis [50]. Because translocation of Bax to mitochondria was observed in AG1478-treated PC-9 cells (K. Takeuchi & F. Ito, unpublished data), AG1478 may exert its apoptotic actions, at least in part, by promoting the translocation of Bax to mitochondria.

Some reports have shown that the activation of the Fas/FasL system may be one of the mechanisms responsible for drug-induced apoptosis in a variety of cancer cells of different histotype [51]. Chang *et al.* recently reported that an increase in Fas protein expression might be the molecular mechanism by which gefitinib induces apoptosis in lung cancer cell lines [52]. Furthermore, it has been reported that c-Jun-dependent FasL expression plays a critical role in the induction of apoptosis by genotoxic agents [53]. To understand the causal relationship between JNK activation and AG1478-induced apoptosis, we need to study whether AG1478 induces the expression of Fas or FasL in PC-9 cells.

Overexpression of MKP-1 inhibited the AG1478-induced JNK activation and also AG1478-induced apoptosis. These results indicate that there is a link between the decreased MKP-1 activity and AG1478-induced apoptosis: MKP-1 expression is controlled by signals downstream of EGFR, and it is downregulated in the presence of an inhibitor of EGFR tyrosine kinase. This downregulation could be followed by JNK activation, triggering the apoptosis pathway.

Understanding the molecular basis of responsiveness to gefitinib is important to identify patients who will have a positive response to this drug. The EGFR gene in tumors from patients with gefitinib-responsive lung cancer was recently examined for mutations, and clustering of mutations was detected in the part of the gene encoding the ATP-binding pocket. Screening for such mutations may identify patients who will have a positive response to the drug. However, this study showed that NSCLC cell line PC-9 was dependent on the MKP-1/JNK pathway for its growth and survival. Thus, sensitivity to gefitinib may be predicted from the detailed analysis of the MKP-1/JNK pathway as described in this study. Although the MKP-1 level in normal cells is low, an increased level of MKP-1 has been found in human ovarian, breast, and prostate cancer [54–56]. Our results suggest that MKP-1 may be a candidate drug target in order to optimize gefitinib-based therapeutic protocols.

Experimental procedures

Materials

EGF (ultra-pure) from mouse submaxillary glands was purchased from Toyobo Co., Ltd (Osaka, Japan). Fetal calf serum came from Gibco (Grand Island, NY, USA). Phenylmethanesulfonyl fluoride, pepstatin A, aprotinin and leupeptin were obtained from Sigma (St Louis, MO, USA). RPMI-1640 medium was from Nissui Pharmaceutical Co., Ltd (Tokyo, Japan). Antibodies used and their sources were: ERK1/2 (pT202/pY204) phospho-specific antibody (clone 20A), JNK(pT183/pY185) phospho-specific antibody

(clone 41), p38 MAPK (pT180/pY182) phospho-specific antibody (clone 36), p38α antibody (clone 27), MKP2 antibody (clone 48) and pan-JNK/SAPK1 antibody (clone 37), from BD Transduction Laboratories (San Jose, CA, USA); MKP-1 antibody (C-19), from Santa Cruz Biotechnology (Santa Cruz, CA, USA); α-tubulin antibody (clone B-5-1-2) and MAP kinase antibody, from Sigma; phospho-SEK1/MKK4 (Ser254/Thr261) antibody and phospho-MKK7 (Ser271/Thr275) antibody, from Cell Signaling Technology (Danvers, MA, USA); swine horseradish peroxidase (HRP)-linked anti-rabbit Ig, from DAKO (Glostrup, Denmark); and sheep HRP-linked anti-mouse Ig, from GE Healthcare UK Ltd (Amersham, UK). Plasmid pcMKP1 was generated from *Homo sapiens* dual-specificity phosphatase 1 cDNA. MGC clone (ID 4794895) purchased from Invitrogen (Carlsbad, CA, USA). The MGC clone had been cloned into pBluscriptR. This clone was digested with *AvaI*, treated with T4 DNA polymerase, ligated to the pcDNA 3.1 mammalian expression vector (Invitrogen) prepared by digestion with *Eco*RV and treated with calf intestinal phosphatase to produce pcMKP1. Plasmid DNA was prepared by standard techniques (Qiagen Plasmid Midi Kit). pBabePuro, a puromycin-resistant vector, was kindly provided by K. Shuai (UCLA, USA). pcDL-SRα296JNK2(VPF), a dominant-negative JNK expression vector, was kindly donated by E. Nishida (Kyoto University, Japan).

Cell culture and transfection

Human non-small cell lung cancer cell line PC-9 was cultured to subconfluence in RPMI-1640 medium supplemented with 5% fetal calf serum and used for all of the experiments. PC-9 cells were plated 24 h before transfection and co-transfected with 8.5 μg of pcDL-SRα 296JNK2(VPF) or pcMKP-1 and 1.5 μg of pBabePuro by using the Lipofectamine reagent, and the transfected cells were selected by exposure to 2.5 mg of puromycin (Sigma) per mL of medium for 3 weeks. Empty vector and pBabePuro were used for co-transfection as a negative control. The expression of JNK protein and MKP-1 protein were verified by immunoblot analysis using anti-(pan-JNK/SAPK1 aa264–415) and anti-(MKP-1) (Santa Cruz Biotechnology), respectively.

Determination of cell viability

The anti-proliferative effect of AG1478 on PC-9 cells was assessed by using a Cell Counting Kit-8 (DOJIN, Kumamoto, Japan) according to the manufacturer's instructions. The Cell Counting Kit-8 is a colorimetric method in which the intensity of the dye is proportional to the number of the viable cells. Briefly, 200 μL of a suspension of PC-9 cells was seeded into each well of a 96-well plate at a density of 2000 cells·well^{-1}. After 48 h, the culture medium was replaced with 100 μL of AG1478 solution at various concentrations. After incubation for 48 h at 37 °C, 10 μL of WST-8 solution was added to each well, and the cells were incubated for a further 40 min at 37 °C. A_{450} was measured using a Bio-Rad microplate reader model 550. Each experiment was performed by using six replicate wells for each drug concentration and was carried out independently three times.

Preparation of cellular lysates and immunoblotting

Preparation of cellular lysates and immunoblotting were performed as described previously [57]. Briefly, cells were lysed with buffer A (20 mM Tris/HCl, pH 7.4, containing 137 mM NaCl, 2 mM EGTA, 5 mM EDTA, 1% Nonidet P-40, 1% Triton X-100, 100 μg·mL^{-1} phenylmethanesulfonyl fluoride, 1 μg·mL^{-1} pepstatin A, 1 μg·mL^{-1} *p*-toluenesulfonyl-L-arginine methyl ester, 2 μg·mL^{-1} leupeptin, 1 mM sodium orthovanadate, 50 mM sodium fluoride and 30 mM $Na_4P_2O_7$). Lysates were then incubated on ice for 30 min, and the insoluble material was cleared by centrifugation. Samples were normalized for protein content and separated by SDS/PAGE, after which they were transferred to an Immobilon-P membrane (Millipore, Bedford, MA, USA) for immunoblotting with antibodies.

Caspase 3 activity assay

Caspase activity was assayed as described previously [57]. Briefly, cells were lysed with buffer A, and the protein concentration in each sample was adjusted to 100 μg·50 μL^{-1} of buffer A. Fifty microliters of 2× Reaction Buffer (0.2 M Hepes/NaOH, pH 7.4, containing 20% sucrose, 0.2% Chaps and 1 mM dithiothreitol) was added to each sample, which was then incubated with Z-DEVD-AFC substrate (50 μM final concentration) at 37 °C for 1 h. The samples were read in a fluorometer (VersaFluor; Bio-Rad) equipped with a 340–380 nm excitation filter (EX 360/40) and 505–515 nm emission filter (EM 510/10).

JNK assay

PC-9 cells were cultured in RPMI-1640 supplemented with 5% fetal calf serum at a density of 6.0×10^5 per 100 mm dish for 2 days and then assayed for JNK activity. JNK assays were performed by using a SAPK/JNK Assay kit (Cell Signaling Technology) according to the manufacturer's specifications. In brief, after various times of treatment with AG1478, adherent cells and floating cells were harvested by centrifugation and washed once in NaCl/P_i. Subsequently, the cells were lysed with lysis buffer (consisting of 20 mM Tris/HCl, pH 7.4, containing 150 mM NaCl, 1 mM EDTA, 1 mM EGTA, 1% Triton X-100, 2.5 mM $Na_4P_2O_7$, 1 mM β-glycerophosphate, 1 mM Na_3VO_4, 1 mM

deltamethrin, 180 nM nodularin, 100 μg·mL^{-1} phenylmethanesulfonyl fluoride, 25 μg·mL^{-1} aprotinin, 25 μg·mL^{-1} leupeptin and 25 μg·mL^{-1} pepstatin), and scraped into microcentrifuge tubes. Extracts were prepared by sonicating each sample on ice (BRANSON SONIFIER 250, Danbury, CT, USA), and insoluble material was removed by microcentrifugation. Soluble fractions were mixed with 2 μg glutathione *S*-transferase c-Jun (1–89) agarose beads (Cell Signaling Technology) and rotated overnight at 4 °C. JNK–c-Jun complexes were collected and washed with lysis buffer followed by kinase buffer, consisting of 25 mM Tris/HCl, pH 7.5, 5 mM β-glycerophosphate, 2 mM Cleland's reagent, 0.1 mM Na_3VO_4 and 10 mM $MgCl_2$. The *in vitro* kinase reaction was initiated by the addition of kinase buffer containing 100 μM ATP, samples were incubated at 30 °C for 45 min, and reactions were terminated by the addition of SDS sample buffer and heating to 95 °C for 5 min. Phosphorylated c-Jun was detected by western blotting using a phospho-specific c-Jun antibody (Cell Signaling Technology).

Hoechst–PI staining

For the study of nuclear morphologic changes induced by AG1478, PC-9 cells were seeded on coverslips, grown to sub-confluence, and treated with AG1478 for the desired times. After fixation with formalin solution, the cells were stained with 10 μM Hoechst33342 and 10 μM PI in 5% fetal calf serum/RPMI. Coverslips were mounted on slides by using Dakocytomation Fluorescent Mounting Medium (DAKO) and observed under a fluorescence microscope (Axioskop; Carl Zeiss, Jena, Germany).

Acknowledgements

We thank Dr K. Shuai for providing the pbabePuro, Dr E. Nishida for pcDL-SRα296JNK2(VPF), a dominant-negative JNK expression vector, and Y. Inoue, Y. Kaji and Y. Hasegawa for technical assistance. This work was supported in part by a grant-in-aid for scientific research from the Ministry of Education, Culture, Sports, Science, and Technology of Japan, and by funding from the Fugaku Trust for Medical Research.

References

1 Burgess AW, Cho HS, Eigenbrot C, Ferguson KM, Garrett TP, Leahy DJ, Lemmon MA, Sliwkowski MX, Ward CW & Yokoyama S (2003) An open-and-shut case? Recent insights into the activation of EGF/ErbB receptors. *Mol Cell* **12**, 541–552.

2 Citri A & Yarden Y (2006) EGF–ERBB signalling: towards the systems level. *Nat Rev Mol Cell Biol* **7**, 505–516.

3 Herbst RS & Bunn PA Jr (2003) Targeting the epidermal growth factor receptor in non-small cell lung cancer. *Clin Cancer Res* **9**, 5813–5824.

4 Nakagawa K, Tamura T, Negoro S, Kudoh S, Yamamoto N, Yamamoto N, Takeda K, Swaisland H, Nakatani I, Hirose M *et al.* (2003) Phase I pharmacokinetic trial of the selective oral epidermal growth factor receptor tyrosine kinase inhibitor gefitinib ('Iressa', ZD1839) in Japanese patients with solid malignant tumors. *Ann Oncol* **14**, 922–930.

5 Gazdar AF, Shigematsu H, Herz J & Minna JD (2004) Mutations and addiction to EGFR: the Achilles 'heal' of lung cancers? *Trends Mol Med* **10**, 481–486.

6 Lynch TJ, Bell DW, Sordella R, Gurubhagavatula S, Okimoto RA, Brannigan BW, Harris PL, Haserlat SM, Supko JG, Haluska FG *et al.* (2004) Activating mutations in the epidermal growth factor receptor underlying responsiveness of non-small-cell lung cancer to gefitinib. *N Engl J Med* **350**, 2129–2139.

7 Paez JG, Jänne PA, Lee JC, Tracy S, Greulich H, Gabriel S, Herman P, Kaye FJ, Lindeman N, Boggon TJ *et al.* (2004) EGFR mutations in lung cancer: correlation with clinical response to gefitinib therapy. *Science* **304**, 1497–1500.

8 Pao W, Miller V, Zakowski M, Doherty J, Politi K, Sarkaria I, Singh B, Heelan R, Rusch V, Fulton L *et al.* (2004) EGF receptor gene mutations are common in lung cancers from 'never smokers' and are associated with sensitivity of tumors to gefitinib and erlotinib. *Proc Natl Acad Sci USA* **101**, 13306–13311.

9 Gilmore AP, Valentijn AJ, Wang P, Ranger AM, Bundred N, O'Hare MJ, Wakeling A, Korsmeyer SJ & Streuli CH (2002) Activation of BAD by therapeutic inhibition of epidermal growth factor receptor and transactivation by insulin-like growth factor receptor. *J Biol Chem* **277**, 27643–27650.

10 Janmaat ML, Kruyt FA, Rodriguez JA & Giaccone G (2003) Response to epidermal growth factor receptor inhibitors in non-small cell lung cancer cells: limited antiproliferative effects and absence of apoptosis associated with persistent activity of extracellular signal-regulated kinase or Akt kinase pathways. *Clin Cancer Res* **9**, 2316–2326.

11 Anderson NG, Ahmad T, Chan K, Dobson R & Bundred NJ (2001) ZD1839 (Iressa), a novel epidermal growth factor receptor (EGFR) tyrosine kinase inhibitor, potently inhibits the growth of EGFR-positive cancer cell lines with or without erbB2 overexpression. *Int J Cancer* **94**, 774–782.

12 Mousser MM, Basso A, Averbuch SD & Rosen N (2001) The tyrosine kinase inhibitor ZD1839 ('Iressa') inhibits HER2-driven signaling and suppresses the growth of HER2-overexpressing tumor cells. *Cancer Res* **61**, 7184–7188.

13 Moulder SL, Yakes FM, Muthuswamy SK, Bianco R, Simpson JF & Arteaga CL (2001) Epidermal growth factor receptor (HER1) tyrosine kinase inhibitor ZD1839 (Iressa) inhibits HER2/neu (erbB2)-overexpressing breast cancer cells *in vitro* and *in vivo*. *Cancer Res* **61**, 8887–8895.

14 Engelman JA, Jänne PA, Mermel C, Pearlberg J, Mukohara T, Fleet C, Cichowski K, Johnson BE & Cantley LC (2005) ErbB-3 mediates phosphoinositide 3-kinase activity in gefitinib-sensitive non-small cell lung cancer cell lines. *Proc Natl Acad Sci USA* **102**, 3788–3793.

15 Ariyama H, Qin B, Baba E, Tanaka R, Mitsugi K, Harada M & Nakano S (2006) Gefitinib, a selective EGFR tyrosine kinase inhibitor, induces apoptosis through activation of Bax in human gallbladder adenocarcinoma cells. *J Cell Biochem* **97**, 724–734.

16 Miyata Y & Nishida E (1999) Distantly related cousins of MAP kinase: biochemical properties and possible physiological functions. *Biochem Biophys Res Commun* **266**, 291–295.

17 Johnson GL & Lapadat R (2002) Mitogen-activated protein kinase pathways mediated by ERK, JNK, and p38 protein kinases. *Science* **298**, 1911–1912.

18 Morrison DK & Davis RJ (2003) Regulation of MAP kinase signaling modules by scaffold proteins in mammals. *Annu Rev Cell Dev Biol* **19**, 91–118.

19 Hibi M, Lin A, Smeal T, Minden A & Karin M (1993) Identification of an oncoprotein- and UV-responsive protein kinase that binds and potentiates the c-Jun activation domain. *Genes Dev* **7**, 2135–2148.

20 Kyriakis JM, Banerjee P, Nikolakaki E, Dai T, Rubie EA, Ahmad MF, Avruch J & Woodgett JR (1994) The stress-activated protein kinase subfamily of c-Jun kinases. *Nature* **369**, 156–160.

21 Kharbanda S, Ren R, Pandey P, Shafman TD, Feller SM, Weichselbaum RR & Kufe DW (1995) Activation of the c-Abl tyrosine kinase in the stress response to DNA-damaging agents. *Nature* **376**, 785–788.

22 Davis RJ (2000) Signal transduction by the JNK group of MAP kinases. *Cell* **103**, 239–252.

23 Chang NS (2001) Hyaluronidase activation of c-Jun N-terminal kinase is necessary for protection of L929 fibrosarcoma cells from staurosporine-mediated cell death. *Biochem Biophys Res Commun* **283**, 278–286.

24 Lamb JA, Ventura JJ, Hess P, Flavell RA & Davis RJ (2003) JunD mediates survival signaling by the JNK signal transduction pathway. *Mol Cell* **11**, 1479–1489.

25 Wada T, Joza N, Cheng HY, Sasaki T, Kozieradzki I, Bachmaier K, Katada T, Schreiber M, Wagner EF, Nishina H *et al.* (2004) MKK7 couples stress signalling to G2/M cell-cycle progression and cellular senescence. *Nat Cell Biol* **6**, 215–226.

26 Camps M, Nichols A & Arkinstall S (2000) Dual specificity phosphatases: a gene family for control of MAP kinase function. *FASEB J* **14**, 6–16.

27 Keyse SM (2000) Protein phosphatases and the regulation of mitogen-activated protein kinase signalling. *Curr Opin Cell Biol* **12**, 186–192.

28 Farooq A & Zhou MM (2004) Structure and regulation of MAPK phosphatases. *Cell Signal* **16**, 769–779.

29 Chen YR, Wang X, Templeton D, Davis RJ & Tan TH (1996) The role of c-Jun N-terminal kinase (JNK) in apoptosis induced by ultraviolet C and gamma radiation. Duration of JNK activation may determine cell death and proliferation. *J Biol Chem* **271**, 31929–31936.

30 Verheij M, Bose R, Lin XH, Yao B, Jarvis WD, Grant S, Birrer MJ, Szabo E, Zon LI, Kyriakis JM *et al.* (1996) Requirement for ceramide-initiated SAPK/JNK signalling in stress-induced apoptosis. *Nature* **380**, 75–79.

31 Sánchez-Pérez I, Martínez-Gomariz M, Williams D, Keyse SM & Perona R (2000) CL100/MKP-1 modulates JNK activation and apoptosis in response to cisplatin. *Oncogene* **19**, 5142–5152.

32 Sordella R, Bell DW, Haber DA & Settleman J (2004) Gefitinib-sensitizing EGFR mutations in lung cancer activate anti-apoptotic pathways. *Science* **305**, 1163–1167.

33 Seimiya H, Mashima T, Toho M & Tsuruo T (1997) c-Jun N-terminal kinase-mediated activation of interleukin-1beta converting enzyme/CED-3-like protease during anticancer drug-induced apoptosis. *J Biol Chem* **272**, 4631–4636.

34 Chu Y, Solski PA, Khosravi-Far R, Der CJ & Kelly K (1996) The mitogen-activated protein kinase phosphatases PAC1, MKP-1, and MKP-2 have unique substrate specificities and reduced activity in vivo toward the ERK2 sevenmaker mutation. *J Biol Chem* **271**, 6497–6501.

35 Franklin CC & Kraft AS (1995) Constitutively active MAP kinase kinase (MEK1) stimulates SAP kinase and c-Jun transcriptional activity in U937 human leukemic cells. *Oncogene* **11**, 2365–2374.

36 Gupta S, Barrett T, Whitmarsh AJ, Cavanagh J, Sluss HK, Dérijard B & Davis RJ (1996) Selective interaction of JNK protein kinase isoforms with transcription factors. *EMBO J* **15**, 2760–2770.

37 Liu Y, Gorospe M, Yang C & Holbrook NJ (1995) Role of mitogen-activated protein kinase phosphatase during the cellular response to genotoxic stress. Inhibition of c-Jun N-terminal kinase activity and AP-1-dependent gene activation. *J Biol Chem* **270**, 8377–8380.

38 Raingeaud J, Gupta S, Rogers JS, Dickens M, Han J, Ulevitch RJ & Davis RJ (1995) Pro-inflammatory cytokines and environmental stress cause p38 mitogen-activated protein kinase activation by dual phosphorylation on tyrosine and threonine. *J Biol Chem* **270**, 7420–7426.